

Upwind schemes for scalar advection-dominated problems in the discrete exterior calculus

Michael Griebel and Christian Rieger and Alexander Schier

Abstract We present the *discrete exterior calculus* (DEC) to solve discrete partial differential equations on discrete objects such as cell complexes. To cope with advection-dominated problems, we introduce a novel stabilization technique to the DEC. To this end, we use the fact that the DEC coincides in special situations with known discretization schemes such as finite volumes or finite differences. Thus, we can carry over well-established upwind stabilization methods introduced for these classical schemes to the DEC. This leads in particular to a stable discretization of the Lie-derivative. We present the numerical features of this new discretization technique and study its numerical properties for simple model problems and for advection-diffusion processes on simple surfaces.

1 Introduction

The *discrete exterior calculus* provides a formalism to describe differential operators on discrete structures such as cell complexes. In the application we have in mind to address in future work is, that we are given a point cloud in the three-dimensional Euclidean space as sample from an unknown surface, i.e. a level-set function. This surface can for instance arise as a free boundary between the two phases in a flow

Michael Griebel
Institute for Numerical Simulation, University of Bonn, Wegelerstr. 6, 53115 Bonn, Germany
Fraunhofer SCAI, Schloss Birlinghoven, 53754 Sankt Augustin, Germany e-mail: griebel@ins.uni-bonn.de

Christian Rieger
Institute for Numerical Simulation, University of Bonn, Wegelerstr. 6, 53115 Bonn, Germany
e-mail: rieger@ins.uni-bonn.de

Alexander Schier
Institute for Numerical Simulation, University of Bonn, Wegelerstr. 6, 53115 Bonn, Germany
e-mail: schier@ins.uni-bonn.de

problem which is modeled by the two-phase Navier-Stokes equation [CGS09]. If this free surface stems from a numerical discretization of a continuous surface, then the number of points is naturally limited by the resolution of the underlying grid which is used for solving the given partial differential equation. This imposes the challenge to describe discrete differential operators and finally a discrete differential equation on the point cloud as surrogate for the continuous differential equation on the surface. To this end, we use the fact that there are many algorithms which can produce a cell complex from a given point cloud, e.g. by using Delaunay triangulations or Voronoi tessellations. This cell complex then serves as a discretization of the free surface in each time step of the physical process.

The main emphasis of the *discrete exterior calculus* is to mimic continuous differential operators in a discrete setting, see [AFW10] for a more abstract theory. As an example, we mention the discrete exterior derivative. As usual, a derivative assigns to each point on the surface a linear form on the tangent space attached to that point. This structure-preserving approach in the discrete exterior calculus is appealing since it does not rely on asymptotic (in the limit of finer and finer grid resolutions) arguments to ensure consistency with the continuous differential operators in the classical sense. The conventional DEC approach, however, suffers from stability issues if it is applied to advection-diffusion-type problems. This is similar to the standard finite element, finite volume or finite difference methods. There, stabilization techniques are necessary like SUPG or upwind, such that a stable discretization results for any advection strength albeit with a somewhat reduced convergence rate.

In this paper, we develop a modification of the DEC which leads to a stable discretization. To this end, we first show that the discrete partial differential equations resulting from the DEC are in simple cases (e.g. flat geometry, regular meshes) equivalent to classical numerical schemes such as finite differences or finite volumes discretizations. Here, finite volumes correspond to the use of dual two-forms whereas finite differences correspond to the use of primal zero-forms. This equivalency of the DEC to a standard scheme then allows us to mimic the well-established numerical upwind schemes from finite volumes and finite differences in the discrete exterior calculus. The resulting approach is new to the best of our knowledge and leads to a stable DEC also for larger advection. This is a desired prerequisite for any two-phase flow problem with an advection-diffusion-reaction process on the free surface.

The remainder of the manuscript is organized as follows: In Section 2, we recall the basics of a cell complex. We will explain how this concept of algebraic topology is related to the more common notions of Delaunay triangulation and Voronoi cells. In Section 3, we review the main objects of the discrete exterior calculus. Here, we do not aim at giving a complete overview but we just focus on the terms needed in the sequel. Our main results are derived in Sections 4.1 and 4.2, namely the equivalence of the discrete exterior calculus with certain numerical schemes in special situations. Based on these observations, we then introduce novel upwind schemes for the discrete exterior calculus. Finally, we give numerical evidence for the con-

vergence and stability properties of our new schemes in Section 5. We conclude this article with some comments in Section 6.

2 From point clouds to cell complexes

In our application, we need to generate a structure which allows to introduce differential operators in a meaningful way based on a given point cloud. Here, the construction of a cell complex from a point cloud is a well known task in topological data analysis, see for instance [EH10, Ede01, Ede14]. We describe the approach as outlined in [Ede98]. The starting point is a point cloud $\mathbb{X}_M = \{p_1, \dots, p_M\} \subset \Omega \subset \mathbb{R}^N$ and the associated (restricted) *Voronoi cells*

$$V_{p:\Omega} := \{x \in \Omega \subset \mathbb{R}^N : \|x - p\|_2 \leq \|x - q\|_2 \text{ for all } q \in \mathbb{X}_M\}, \quad p \in \mathbb{X}_M.$$

To introduce an abstract simplicial complex, let $\mathcal{A} = \{A_1, \dots, A_n\}$ be a finite collection of some sets. Then, the nerve of \mathcal{A} is defined as

$$\text{Nrv } \mathcal{A} := \left\{ \mathcal{B} \subseteq \mathcal{A} : \bigcap_{A_j \in \mathcal{B}} A_j \neq \emptyset \right\}.$$

Note here that we denote the initial sets of \mathcal{A} by A_j and the collection of any of the subsets of \mathcal{A} by calligraphic letters. Note also the important property that $\mathcal{C} \subseteq \mathcal{B}$ and $\mathcal{B} \in \text{Nrv } \mathcal{A}$ implies $\mathcal{C} \in \text{Nrv } \mathcal{A}$. This makes $\text{Nrv } \mathcal{A}$ an abstract simplicial complex. We assume to have an injective function

$$\phi : \mathcal{A} \rightarrow \mathbb{R}^{n_{\mathcal{A}}}, \quad A_j \mapsto \phi(A_j),$$

where $n_{\mathcal{A}} \in \mathbb{N}$ is an arbitrary natural number. This map can be extended to arbitrary $\mathcal{B} \in \text{Nrv } \mathcal{A}$ with $\mathcal{B} = \{A_{j_1}, \dots, A_{j_n}\}$ via

$$\begin{aligned} \phi(\mathcal{B}) &= \phi(\{A_{j_1}, \dots, A_{j_n}\}) := \text{conv}[\phi(A_{j_1}), \dots, \phi(A_{j_n})] \\ &:= \left\{ y \in \mathbb{R}^{n_{\mathcal{A}}} : y = \sum_{i=1}^n \alpha_i \phi(A_{j_i}), 0 \leq \alpha_i \text{ for all } 1 \leq i \leq n \text{ and } \sum_{i=1}^n \alpha_i = 1 \right\} \subset \mathbb{R}^{n_{\mathcal{A}}} \end{aligned}$$

such that

$$\phi(\mathcal{B}) \cap \phi(\mathcal{C}) = \phi(\mathcal{B} \cap \mathcal{C}) \quad \text{for all } \mathcal{B}, \mathcal{C} \in \text{Nrv } \mathcal{A}.$$

$$\mathcal{H}_{\mathcal{A}} := \{ \text{conv}[\phi(\mathcal{B})] = \text{conv}[\phi(B_{j_1}), \dots, \phi(B_{j_n})] : \mathcal{B} \subset \mathcal{A} \} \quad (1)$$

a *simplicial complex* and the tuple $(\mathcal{H}_{\mathcal{A}}, \phi)$ a *geometric realization* of $\text{Nrv } \mathcal{A}$. The underlying space is defined as $|\mathcal{H}_{\mathcal{A}}|_{\text{sp}} := \bigcup \mathcal{H}_{\mathcal{A}}$. The (restricted) *Delaunay complex*

of \mathbb{X}_M is the geometric realization of $\text{Nrv}V_{p:\Omega}$ and the map is $\phi : V_{p:\Omega} \mapsto p$. This makes $n_{\mathcal{A}} = N$. In particular, we recover the standard definition of a simplex. From now on, we mainly follow [DHLM05] and [Hir03].

Definition 1. A k -simplex $\sigma^{(k)}$ for $N \geq k \in \mathbb{N}$ in \mathbb{R}^N is the convex hull of $k + 1$ affinely independent vectors $v_i \in \mathbb{R}^N$, i.e.,

$$\sigma^{(k)} = [v_0, \dots, v_k] = \left\{ \sum_{i=0}^k \alpha_i v_i, \left| \alpha_i \geq 0, \text{ for } i = 0, \dots, k \text{ and } \sum_{i=0}^k \alpha_i = 1 \right. \right\}.$$

The points v_0, \dots, v_k are called the *vertices* of the simplex, and the number k is called the *dimension* of the simplex. A simplex $\sigma^{(\ell)}$ spanned by a (proper) subset of cardinality $0 \leq \ell \leq k$ of the vertices of $\sigma^{(k)}$ is a (proper) ℓ -*face* of $\sigma^{(k)}$. We write $\sigma^{(\ell)} \prec \sigma^{(k)}$, if $\sigma^{(\ell)}$ is a proper ℓ -face of $\sigma^{(k)}$ for some $0 \leq \ell \leq k$. We define the set of faces of a 0-simplex $\sigma^{(0)}$ as \emptyset .

Moreover, the Delaunay complex as simplicial complex has the following form:

Definition 2. A *simplicial complex* K of dimension $n \leq N$ is a collection of $0, \dots, n$ -simplices in \mathbb{R}^N , such that

- The faces of each simplex of K are in K .
- Two simplices have no intersection or they intersect at a common face.

We call a simplicial complex K of dimension n *manifold-like* if the polytope of K is a \mathcal{C}^0 -manifold.

We can orient simplices using the order of their vertices.

Definition 3. Let $\sigma^{(k)}$ be a k -simplex, and fix the order of its vertices. Every even permutation of the vertices induces the same orientation, while an odd permutation reverses the sign of the orientation. For a 0-simplex we define the orientation as positive, for n -simplices we assume that the orientation is given.

From the orientation of a simplex, we can induce an orientation on its faces.

Definition 4. Let $\sigma^{(k)} = [v_0, \dots, v_k]$ be an oriented simplex with $k \geq 1$. Consider the face $\sigma^{(k-1)}[v_0, \dots, \hat{v}_i, \dots, v_k]$, where the vertex \hat{v}_i is omitted. This face has a positive orientation induced by $\sigma^{(k)}$ if i is even, otherwise its induced orientation is negative. Two k -simplices with $k > 0$ are *adjacent*, if they share a common $(k - 1)$ -face.

Finally, we will employ the following notion of a subcomplex.

Definition 5. Let K be a simplicial complex of dimension n , and let L be a subset of K that is a simplicial complex itself. Then L is called a subcomplex of K . For $k < n$, we call the subcomplex which contains all simplices of K of dimension at most k the k -*skeleton* of K .

2.1 Dual Complex

In this subsection, K always denotes an oriented manifold-like simplicial complex. We introduce the dual complex. Loosely speaking, a simplicial complex defines a dual complex $\star K$, by using the centers c_i of the n -simplices of the primal complex as vertex set and then connecting adjacent centers, where, on the boundary of the complex, we add the centers of the boundary faces as dual vertices. A simple example in the two-dimensional case is given in Figure 1.

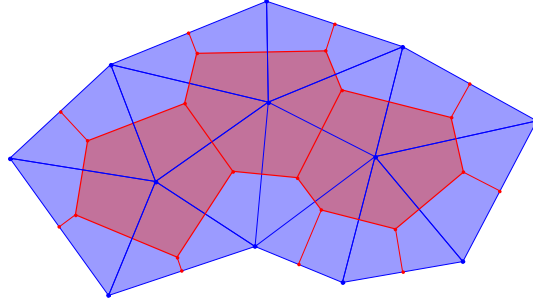


Fig. 1: A two-dimensional simplicial complex with its dual cells

We will later on use a circumcentric dual complex.

Definition 6. The *circumcenter* of a k -simplex $\sigma^{(k)} = [v_0, \dots, v_k]$ is given by the center of its k -circumsphere, which is the unique k -sphere that has the vertices v_0, \dots, v_k on its surface. Equivalently, the circumcenter is the unique point in the k -dimensional affine space that contains the k -simplex, which is equidistant to the $k+1$ vertices of the simplex. We denote the circumcenter of a simplex $\sigma^{(k)}$ with $c_i = c(\sigma_i^{(k)})$.

We will need an additional assumption on the primal simplicial complex.

Definition 7. An n -simplex with $n \leq N$ is called *well-centered* if its circumcenter lies in its interior. A simplicial complex is called *well-centered* if each simplex in the complex is well-centered.

We are now in the position to define the dual cells.

Definition 8. Let K be a well-centered manifold-like simplicial complex of dimension n , and let $\sigma^{(k)}$ be one of the k -simplices of K with $0 \leq k \leq n \leq N$. We define the *dual cell* $\star\sigma^{(k)}$ as

$$\star\sigma^{(k)} := \bigcup_{r=0}^{n-k} \bigcup_{\sigma^{(k)} \prec \sigma_1 \prec \dots \prec \sigma_r} [c(\sigma^{(k)}), c(\sigma_1), \dots, c(\sigma_r)] \quad (2)$$

The *dual cell complex* $\star K$ is the union of all dual cells $\star\sigma^{(k)}$, $0 \leq k \leq n \leq N$.

We note that, in general, a dual cell is not a simplex. See Figure 1 for an example of dual cells of the simplicial complex.

To conclude this section, note that we will work with Voronoi cells and Delaunay triangulations (see [Aur91]). To this end, recall some basic relations (see [KA03]), which are common also in the numerical treatment of partial differential equations. The following facts are well established: In a Delaunay mesh with well-centered cells, the circumcentric dual cells of the vertices are their Voronoi regions. See also [VHG⁺13] for more details on well-centered triangulations. An edge connecting the circumcenters of two adjacent k -simplices of a well-centered mesh intersects the common $(k-1)$ -face at its circumcenter and is perpendicular to the face.

3 The Discrete Exterior Calculus

We now want to employ the discrete exterior calculus (DEC) to solve PDEs. It is based on the representation of the domain of the partial differential equation as underlying space $|K|_{\text{sp}}$ of a cell-complex K . We first introduce the basic operations of the discrete exterior calculus. Here, we follow [DhLM05] and [Hir03]. We start with an oriented and manifold-like simplicial complex K of dimension $n \leq N$ in \mathbb{R}^N and denote its k -simplices by $\sigma^{(k)}$. The space of k -chains of k -simplices is given by the basic elements

$$C_k(K) := C_k(K; \mathbb{Z}) := \left\{ \sum_{j=1}^{N_k} \alpha_j \sigma_j^{(k)} : \alpha_j \in \mathbb{Z} \right\}, \quad (3)$$

where we use $N_k \in \mathbb{N}$ to denote the number of k -simplices. $C_k(K; \mathbb{Z})$ is naturally equipped with an Abelian group structure (with addition). The space of discrete k -forms (co-chains) is the dual space of the k -chains, i.e., the space of homomorphisms from the (group) of k -chains to the usual additive group $(\mathbb{R}, +)$. Precisely, we have

$$C^k(K) := \text{Hom}(C_k(K; \mathbb{Z}), \mathbb{R}).$$

Naturally, a k -form is uniquely defined by its evaluation on the elements of $C_k(K)$. This leads to the idea that one simply has to store a list of all evaluations of a k -form

$$C^k(K) \ni \omega^k \leftrightarrow (\langle \omega^k, \sigma_1^k \rangle, \dots, \langle \omega^k, \sigma_{N_k}^k \rangle)^\top \in \mathbb{R}^{N_k}, \quad (4)$$

where the evaluation of a k -form on a k -chain is written by the bilinear pairing $\langle \omega^k, \sigma^{(k)} \rangle \in \mathbb{R}$. The same constructions can be applied to the dual cell complex $\star K$. We denote the Abelian group of k -chains on the dual complex by

$$C_k(\star K) := C_k(\star K; \mathbb{Z}) := \left\{ \sum_{j=1}^{N_k} \alpha_j \star \sigma_j^{(k)} : \alpha_j \in \mathbb{Z} \right\}.$$

Furthermore, we denote the space of k -forms on the dual complex as

$$C^k(\star K_d) := \text{Hom}(C^k(\star K), \mathbb{R}).$$

There is a natural chain complex, i.e., an homomorphism $\partial_k : C_k(K) \rightarrow C_{k-1}(K)$, such that

$$0 \longrightarrow C_N(K) \xrightarrow{\partial_N} C_{N-1}(K) \xrightarrow{\partial_{N-1}} \dots \xrightarrow{\partial_1} C_0(K) \longrightarrow 0,$$

with $\text{Im}(\delta_{k+1}) \subset \ker(\delta_k)$, i.e., $\delta_k \circ \delta_{k+1} \equiv 0$ for all $0 \leq k \leq N-1$. Furthermore, there is also an associated co-chain complex, i.e., a homomorphism $\delta_k : C^k(K) \rightarrow C^{k+1}(K)$ such that

$$0 \longleftarrow C^N(K) \xleftarrow{\delta_N} C^{N-1}(K) \xleftarrow{\delta_{N-1}} \dots \xleftarrow{\delta_1} C^0(K) \longleftarrow 0.$$

We now identify a k -simplex σ^k with its ordered set of vertices $[v_0, \dots, v_k]$. Then, we get a mapping from the simplex to a $(k-1)$ -chain of its boundary simplices

$$\partial_k \sigma^k = \partial_k([v_0, \dots, v_k]) = \sum_{i=0}^k (-1)^i [v_0, \dots, \hat{v}_i, \dots, v_k] \quad (5)$$

where \hat{v}_i means that the vertex v_i is omitted.

Definition 9. The boundary operator $\partial_k : C_k(K) \rightarrow C_{k-1}(K)$ induces as formal adjoint with respect to the bilinear pairing $\langle \cdot, \cdot \rangle : C^k(K) \times C_k(K) \rightarrow \mathbb{R}$ the operator $\mathbf{d} : C^k(K) \rightarrow C^{k+1}(K)$. Precisely, we have

$$\langle \mathbf{d}\omega^k, \sigma^{k+1} \rangle := \langle \omega^k, \partial \sigma^{k+1} \rangle \quad (6)$$

for all $\sigma^{k+1} \in C_{k+1}(K)$. The operator \mathbf{d} is called co-boundary operator and its definition can be seen as a variant of Stokes' theorem.

By construction, we have $\partial_k \circ \partial_{k+1} \equiv 0$. For our calculus, we need some more specific operations. They are defined in the following.

Definition 10. The discrete Hodge Star operator is a map $\star : C^k(K) \rightarrow C^k(\star K)$. For a k -cochain ω^k it is defined as

$$\frac{1}{|\sigma^k|} \langle \omega^k, \sigma^k \rangle = \frac{1}{|\star \sigma^k|} \langle \star \omega^k, \star \sigma^k \rangle. \quad (7)$$

for all k -simplices σ^k .

We have the following identity

$$\star(\star \omega^k) = (-1)^{k(n-k)} \omega^k, \quad (8)$$

for all k -cochains ω^k . Furthermore, we also have the analogue relation for k -chains, i.e.,

$$\star(\star\sigma^{(k)}) = (-1)^{k(n-k)} \sigma^{(k)}. \quad (9)$$

A further necessary ingredient is an operation which allows to glue together k -forms. This operation is usually called *wedge product*.

Definition 11. Given a primal discrete k -form $\alpha^k \in C^k(K)$ and a primal discrete l -form $\beta^l \in C^l(K)$, the discrete *primal-primal wedge product* $\wedge : C^k(K) \times C^l(K) \rightarrow C^{k+l}(K)$ defined by the evaluation on a $(k+l)$ -simplex $\sigma^{k+l} = [v_0, \dots, v_{k+l}]$ is given by

$$\langle \alpha^k \wedge \beta^l, \sigma^{k+l} \rangle := \frac{1}{(k+l)!} \sum_{\tau \in S_{k+l+1}} \text{sgn}(\tau) \frac{|\sigma^{k+l} \cap \star v_{\tau(k)}|}{|\sigma^{k+l}|} \langle \alpha^k \smile \beta^l, \tau(\sigma^{k+l}) \rangle$$

where S_{k+l+1} is the permutation group and its elements are thought of as permutations of the numbers $0, \dots, (k+l+1)$. Here, we define $\star v_{\tau(k)}$ as the dual cell corresponding to the 0-simplex $[v_{\tau(k)}]$ and the notation $\tau(\sigma^{k+l})$ stands for the simplex $[v_{\tau(0)}, \dots, v_{\tau(k+l)}]$. Moreover, the \smile operator is defined by the evaluation of $\alpha \smile \beta$ on a $(k+l)$ -simplex as

$$\langle \alpha^k \smile \beta^l, \tau(\sigma^{k+l}) \rangle := \langle \alpha^k, [v_{\tau(0)}, \dots, v_{\tau(k)}] \rangle \langle \beta^l, [v_{\tau(k)}, \dots, v_{\tau(k+l)}] \rangle.$$

For example, we get for the special case of a 1-form α^1 and a 0-form β^0 :

$$\begin{aligned} \langle \alpha^1 \wedge \beta^0, [v_0, v_1] \rangle = & \quad (10) \\ & \left[\frac{|[v_0, v_1] \cap \star[v_1]|}{|[v_0, v_1]|} \langle \alpha^1, [v_0, v_1] \rangle \langle \beta^0, [v_1] \rangle \right] \\ & - \left[\frac{|[v_0, v_1] \cap \star[v_0]|}{|[v_0, v_1]|} \langle \alpha^1, [v_1, v_0] \rangle \langle \beta^0, [v_0] \rangle \right], \end{aligned}$$

see also [MHR16, Eq. (16)] for this expression. Now, in order to introduce an upwind-effect into the formalism of discrete exterior calculus, we have to modify the geometric weight factors $\frac{|\sigma^{k+l} \cap \star v_{\tau(k)}|}{|\sigma^{k+l}|}$. To this end, we replace $\frac{|[v_0, v_1] \cap \star[v_1]|}{|[v_0, v_1]|}$ by some $r_{0,1}^{(1)} \in [0, 1]$, and $\frac{|[v_0, v_1] \cap \star[v_0]|}{|[v_0, v_1]|}$ by $1 - r_{0,1}^{(1)}$, see Figure 2 for an illustration. This gives

$$\begin{aligned} \langle \alpha^1 \wedge_{\text{up}} \beta^0, [v_0, v_1] \rangle & \quad (11) \\ := & \left[r_{0,1}^{(1)} \langle \alpha^1, [v_0, v_1] \rangle \langle \beta^0, [v_1] \rangle \right] - \left[(1 - r_{0,1}^{(1)}) \langle \alpha^1, [v_1, v_0] \rangle \langle \beta^0, [v_0] \rangle \right], \end{aligned}$$

where we will provide some choices for the term $r_{0,1}^{(1)}$ in the sequel.

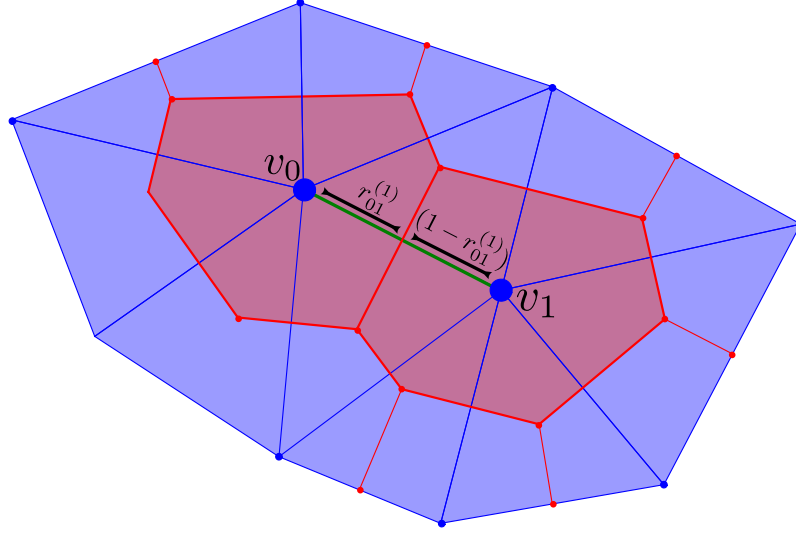


Fig. 2: Sketch of weight factor

Furthermore, we need an operator which allows to assign a 1-form to a given vector field. Loosely speaking, a vector field on a dual cell complex $\star K$ is a smooth map $\mathbf{v} : |\star K|_{\text{sp}} \rightarrow \mathbb{R}^N$. The operator which assigns a 1-form to \mathbf{v} is called *flat operator* and the resulting form is denoted by v^\flat .

In the discrete setting, there are several choices of the flat operator depending on the discretization of the vector field, the areas over which we want to interpolate the field and if we want to evaluate v^\flat on primal or dual edges. We refer to [Hir03, Chapter 5] for a detailed discussion of the different flats. See also [NNPV16] for another version of a discrete flat. In the following, we will use the flat operator \flat_{dpp} for a dual vector field projected on primal edges with interpolation over primal volumes.

Definition 12. The *dual-primal-primal flat operator* \flat_{dpp} is given by the evaluation of a vector field \mathbf{v} , which is assumed to be piecewise constant inside 2-simplices, on a primal 1-simplex $\sigma^{(1)} = [\sigma_l^{(0)}, \sigma_r^{(0)}]$. We have

$$\langle v^{\flat_{dpp}}, \sigma^{(1)} \rangle := \sum_{\sigma^{(2)} \supset \sigma^{(1)}} \frac{|\star \sigma^{(1)} \cap \sigma^{(2)}|}{|\sigma^{(1)}|} \mathbf{v}(\sigma^{(2)}) \cdot (\sigma_r^{(0)} - \sigma_l^{(0)}), \quad (12)$$

where $\sigma_r^{(0)} - \sigma_l^{(0)} \in \mathbb{R}^2$ denotes the vector corresponding to the edge $\sigma^{(1)} = [\sigma_l^{(0)}, \sigma_r^{(0)}]$.

The dual-primal-primal flat operator is also well defined on curved meshes, which is not automatically true for all the other choices of flats in the discrete setting.

Finally, we define the contraction of a vector field and a k -form.

Definition 13. Let $\mathbf{v} : |\star K|_{\text{sp}} \rightarrow \mathbb{R}^N$ be a given smooth vector field and let $\omega^{(k)} \in C^k(\star K)$ be a dual $0 \leq k \leq n \leq N$ -form. Then, we define the *contraction*

$$i_{\mathbf{v}}\omega^{(k)} := (-1)^{k(n-k)} \star \left(\star \omega^{(k)} \wedge v^{\flat dpp} \right) \in C^{k-1}(\star K).$$

This algebraic approach is also used in [MHR16, Eq. (9)]. There is also a more geometrically motivated definition of the extrusion of a manifold with a flow. Theorem 3 gives a relation to the contraction.

Definition 14. Given a manifold M , a k -submanifold S and a vector field β on M , we call the manifold obtained by sweeping S along the flow of β for a time t the *extrusion* of S by β for a time t and denote it by $\text{extr}_{\beta}(S, t)$. The manifold S carried by the flow for a time t will be denoted by $\phi_{\beta}^t(S)$, see [DhLM05, Definition 10.1]. This extrusion $\text{extr}_{\beta}(S, T)$ is the union of all Manifolds $\phi_{\beta}^t(S)$ with $t \in [0, T]$:

$$\text{extr}_{\beta}(S, T) := \bigcup_{t=0}^T \phi_{\beta}^t(S)$$

We shall use this definition in Theorem 3.

The different operators introduced so far will be used in the following to define partial differential equations on simplicial complexes. For details on the implementation of such methods, see also [BH].

4 Relation between the DEC and other numerical schemes

In this section, we consider an elliptic partial differential equation with $\alpha > 0$ of the following form

$$\begin{aligned} -\alpha \Delta u + \nabla \cdot (\mathbf{v}u) + cu &= f && \text{on } \Omega, \\ u &= 0 && \text{on } \partial\Omega, \end{aligned} \quad (13)$$

where $\mathbf{v} : \Omega \rightarrow \mathbb{R}^2$ is a given vector field. Note that this is the essential step in order to treat two-dimensional manifolds. The DEC has already proven to be appropriate for solving differential equations in many different situations. To name a few: For Darcy's equation, see [HNC15]. For Navier-Stokes, see [MHR16] and also [NRV16]. For an energy minimization of Frank-Oseen-type, see [NNPV16]. In order to compare conventional numerical schemes for the discretization of this partial differential equation with schemes based on the discrete exterior calculus, we start with the points (primal vertices) \mathbb{X}_{N_0} and form the restricted Voronoi cells $V_{p;\Omega}$. The corresponding Delaunay triangulation yields the primal 2-simplices. We recall the geometric setting in Figure 3.

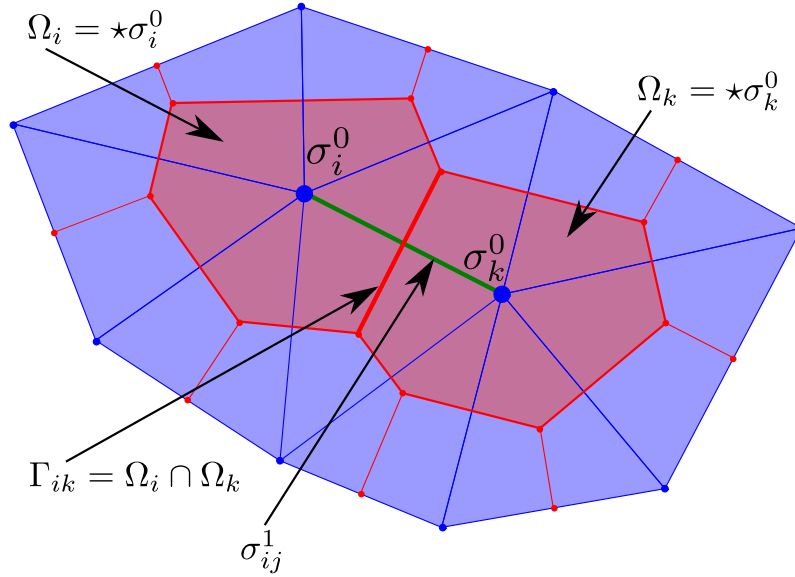


Fig. 3: Sketch of internal nodes and the corresponding primal and dual complexes

We first discuss finite volumes schemes but use the geometric terms from the cell complexes. Thus, we make the discussion in [MMP⁺11, Section 4.1] mathematically precise and provide an upwind scheme for the discrete exterior calculus.

4.1 Finite volumes

As a classical discretization, we consider the finite volume method (FVM) in the two-dimensional case as described in [KA03, Chapter 6] and aim at an interpretation in the DEC formalism. To be precise, we use a dual grid with a *cell-centered* finite volume method approach as described in [Bey98, section 4.1.2] employing the perpendicular bisector method [Bey98, Definition 4.1.4]. This is equivalent to the circumcentric dual grid of the DEC, as the intersection of the perpendicular bisectors inside a triangle is just the circumcenter. Using the notation from Section 2, we denote the Voronoi cell complex with $\star K$ and the primal simplicial complex with K . The numerical discretization with finite volumes uses piecewise linear polynomials on the Delaunay triangles as trial functions and piecewise constant functions on the Voronoi cells as test functions. Given a (primal) vertex or 0-simplex $\sigma_i^{(0)}$, we denote its Voronoi cell by $\star\sigma_i^{(0)}$. Then, we have the finite volume discretization as: Find $u_h \in \mathbb{P}_1(K)$ such that

$$\int_{\star\sigma_i^{(0)}} \alpha \Delta u_h dx - \int_{\star\sigma_i^{(0)}} \nabla \cdot (\mathbf{v}u_h) dx + \int_{\star\sigma_i^{(0)}} cu_h dx = \int_{\star\sigma_i^{(0)}} f dx \quad (14)$$

for all internal control volumes. We now describe for each of the integrals in equation (14) how it is numerically evaluated. Following [KA03, p. 306], we approximate the reaction term and the right hand side with the midpoint rule, i.e.

$$\int_{\star\sigma_i^{(0)}} f dx \approx |\star\sigma_i^{(0)}| f(\sigma_i^{(0)}) \quad \text{and} \quad \int_{\star\sigma_i^{(0)}} r u dx \approx |\star\sigma_i^{(0)}| r(\sigma_i^{(0)}) u(\sigma_i^{(0)}). \quad (15)$$

For the advection and diffusion terms, we use the divergence theorem

$$\int_{\star\sigma_i^{(0)}} \nabla \cdot (\alpha \nabla u - (\mathbf{v}u)) dx = \int_{\partial\star\sigma_i^{(0)}} \alpha \mathbf{v} \cdot \nabla u d\sigma - \int_{\partial\star\sigma_i^{(0)}} \mathbf{v} \cdot (\mathbf{v}u) d\sigma, \quad (16)$$

where \mathbf{v} denotes the outer unit normal to $\partial\star\sigma_i^{(0)}$. The boundary of a Voronoi cell can be decomposed into faces which are dual edges. We thus can write

$$\partial\star\sigma_i^{(0)} = \bigcup_{\sigma_i^{(0)} \prec \sigma^{(1)}} \star \left(\partial\sigma^{(1)} \setminus \{\sigma_i^{(0)}\} \right) \cap \star\sigma_i^{(0)} = \bigcup_{\partial\star\sigma_i^{(0)} \prec \star\sigma_k^{(0)}} \star\sigma_k^{(0)} \cap \star\sigma_i^{(0)}.$$

This is the reason why usually a dual edge $\Gamma_{i,k}$ is denoted by two indices indicating the two dual control volumes which are used to define this straight part of the boundary of the dual cell. We get

$$\begin{aligned} & \int_{\partial\star\sigma_i^{(0)}} \alpha \mathbf{v} \cdot \nabla u d\sigma - \int_{\partial\star\sigma_i^{(0)}} \mathbf{v} \cdot (\mathbf{v}u) d\sigma \\ &= \sum_{\partial\star\sigma_i^{(0)} \prec \star\sigma_k^{(0)}} \left[\int_{\star\sigma_k^{(0)} \cap \star\sigma_i^{(0)}} \alpha \mathbf{v} \cdot \nabla u d\sigma - \int_{\star\sigma_k^{(0)} \cap \star\sigma_i^{(0)}} \mathbf{v} \cdot (\mathbf{v}u) d\sigma \right]. \end{aligned}$$

Furthermore, we make the following approximations (using a constant $\alpha > 0$): We set

$$\alpha = \alpha|_{\sigma_k^{(0)} \cap \star\sigma_i^{(0)}} = \mu_{i,k}, \quad \mathbf{v} \cdot \mathbf{v}|_{\star\sigma_k^{(0)} \cap \star\sigma_i^{(0)}} \approx \gamma_{i,k},$$

which yields the following approximation to the boundary integrals

$$\begin{aligned} & \sum_{\partial\star\sigma_i^{(0)} \prec \star\sigma_k^{(0)}} \left[\int_{\star\sigma_k^{(0)} \cap \star\sigma_i^{(0)}} \alpha \mathbf{v} \cdot \nabla u d\sigma - \int_{\star\sigma_k^{(0)} \cap \star\sigma_i^{(0)}} \mathbf{v} \cdot (\mathbf{v}u) d\sigma \right] \\ & \approx \sum_{\partial\star\sigma_i^{(0)} \prec \star\sigma_k^{(0)}} \left[\mu_{ij} \int_{\star\sigma_k^{(0)} \cap \star\sigma_i^{(0)}} \mathbf{v} \cdot \nabla u d\sigma - \gamma_{ij} \int_{\star\sigma_k^{(0)} \cap \star\sigma_i^{(0)}} u d\sigma \right]. \end{aligned}$$

The gradient and hence the normal derivatives are discretized by standard difference quotients

$$(\mathbf{v} \cdot \nabla u)|_{\star\sigma_k^{(0)} \cap \star\sigma_i^{(0)}} \approx \frac{u(\sigma_k^{(0)}) - u(\sigma_i^{(0)})}{|[\sigma_i^{(0)}, \sigma_i^{(0)}]|}.$$

The most delicate term is the advection since this is crucial for the stability of the resulting numerical scheme. We set

$$u|_{\star\sigma_k^{(0)} \cap \star\sigma_i^{(0)}} \approx r_{i,k}u(\sigma_k^{(0)}) + (1 - r_{i,k})u(\sigma_i^{(0)}) \quad (17)$$

with $r_{i,k} \in [0, 1]$ as parameter, which then allows for upwind schemes. In summary, we obtain the following discretization of (14)

$$\begin{aligned} & \sum_{\partial\star\sigma_i^{(0)} \prec \star\sigma_k^{(0)}} |\star\sigma_k^{(0)} \cap \star\sigma_i^{(0)}| \mu_{i,k} \frac{u(\sigma_k^{(0)}) - u(\sigma_i^{(0)})}{|v|} \\ & - \sum_{\partial\star\sigma_i^{(0)} \prec \star\sigma_k^{(0)}} |\star\sigma_k^{(0)} \cap \star\sigma_i^{(0)}| \gamma_{ij} [r_{ij}u(\sigma_i^{(0)}) + (1 - r_{ij})u(\sigma_k^{(0)})] \\ & + |\star\sigma_i^{(0)}| r(\sigma_i^{(0)}) u(\sigma_i^{(0)}) = |\star\sigma_i^{(0)}| f(\sigma_i^{(0)}) \end{aligned} \quad (18)$$

Note again that this scheme is parametrized with $r_{i,k} \in [0, 1]$. These parameters can now be used to obtain a stable discretization provided that the $r_{i,k}$ are chosen appropriately.

Equivalence to the DEC method

Now, we derive a DEC formulation of the advection-diffusion equation. Then, we will show that the discrete partial differential equation is indeed equivalent to the finite volume discretization. The Laplacian is a well-studied object in the discrete exterior calculus We will therefore mainly focus on the advection term which is modeled by the Lie-advection in the discrete exterior calculus We first follow [Heu11] and get for a vector field $\beta : \Omega \rightarrow \mathbb{R}^2$ the expression

$$L_\beta \omega = i_\beta d\omega + di_\beta \omega$$

for the Lie advection of a differential k -form, where i_β is the contraction (see Definition 13) of the differential form and a vector field which yields a $(k - 1)$ -form. We will now show that the FVM is equivalent to solving the advection-diffusion-reaction PDE using dual 2-forms. For detailed definitions in the continuous context, see [Heu11, Eqns. 2.23 & 2.24]. We note here only the important equivalence

$$L_\beta \omega \sim \begin{cases} \beta \cdot \nabla u, & k = 0, \\ \nabla \cdot (\beta u), & k = 2. \end{cases} \quad (19)$$

Hence, we expect to deal with differential 2-form if we study a discretization of (13). Since the testing is done on dual 2-cells, we have to use dual 2-forms. We use the subscript d to denote the fact that the forms are dual. We solve for the dual discrete differential 2-form ω_d^2 , which corresponds to the integrated quantity $\int_{\star\sigma_i^{(0)}} u dx dy$ from the finite volume approach. The relation $\omega_d^2 = \star_0 \omega^0$ defines the mapping between the integral and the piecewise constant function inside the control volume.

Theorem 1. *Let $\omega_d^2, \eta_d^2 \in C^2(\star K)$ be dual 2-forms, $\alpha \geq 0$ and $c \in \mathbb{R}$ given constants and $\mathbf{v} : |\star K| \rightarrow \mathbb{R}^2$ a vector field. We consider*

$$\alpha \langle \mathbf{d} \star \mathbf{d} \star \omega_d^{(2)}, \star[\sigma_i^{(0)}] \rangle + \langle \mathbf{d} \mathbf{i}_{\mathbf{v}} \omega_d^{(2)}, \star[\sigma_i^{(0)}] \rangle + c \langle \omega_d^{(2)}, \star[\sigma_i^{(0)}] \rangle = \langle \eta_d^2, \star[\sigma_i^{(0)}] \rangle. \quad (20)$$

By setting $u := \star \omega_d^2$, $f = \star \eta_d^2$ and $r_{i,j} = r_{i,j}^{(1)}$ according to (24), we obtain that (20) is equivalent to (14).

Proof. We directly compute

$$\langle \eta_d^{(2)}, \star[\sigma_i^{(0)}] \rangle = \langle \star \eta_d^{(2)}, [\sigma_i^{(0)}] \rangle = |\star[\sigma_i^{(0)}]| f(\sigma_i^{(0)}). \quad (21)$$

Also, by formula (8), we have

$$\begin{aligned} \langle \omega_d^2, \star[\sigma_i^{(0)}] \rangle &= (-1)^{2 \cdot (2-2)} \langle \star \star \omega_d^{(2)}, \star[\sigma_i^{(0)}] \rangle = \langle \star \omega_d^{(2)}, [\sigma_i^{(0)}] \rangle \\ &= \left| \star[\sigma_i^{(0)}] \right| \langle \star \omega_d^{(2)}, \sigma_i^{(0)} \rangle \end{aligned} \quad (22)$$

using (7). For the diffusion term, we get

$$\begin{aligned} \langle \mathbf{d} \star \mathbf{d} \star \omega_d^{(2)}, \star[\sigma_i^{(0)}] \rangle &= \langle \star \mathbf{d} \star \omega_d^{(2)}, \partial \star[\sigma_i^{(0)}] \rangle \\ &= \langle \star \mathbf{d} \star \omega_d^{(2)}, (-1)^{1(2-1)} \star \star \partial \star[\sigma_i^{(0)}] \rangle \\ &= (-1) \sum_{[\sigma_i^{(0)}] \prec [\sigma_k^{(0)}, \sigma_i^{(0)}]} \frac{|\star[\sigma_i^{(0)}] \cap \star[\sigma_k^{(0)}]|}{|[\sigma_k^{(0)}, \sigma_i^{(0)}]|} \langle \mathbf{d} \star \omega_d^{(2)}, [\sigma_k^{(0)}, \sigma_i^{(0)}] \rangle \\ &= (-1) \sum_{[\sigma_i^{(0)}] \prec [\sigma_k^{(0)}, \sigma_i^{(0)}]} \frac{|\star[\sigma_i^{(0)}] \cap \star[\sigma_k^{(0)}]|}{|[\sigma_k^{(0)}, \sigma_i^{(0)}]|} \langle \star \omega_d^{(2)}, \partial[\sigma_k^{(0)}, \sigma_i^{(0)}] \rangle \\ &= (-1) \sum_{[\sigma_i^{(0)}] \prec [\sigma_k^{(0)}, \sigma_i^{(0)}]} \left| \star[\sigma_i^{(0)}] \cap \star[\sigma_k^{(0)}] \right| \frac{\langle \star \omega_d^{(2)}, [\sigma_k^{(0)}] \rangle - \langle \star \omega_d^{(2)}, [\sigma_i^{(0)}] \rangle}{|[\sigma_k^{(0)}, \sigma_i^{(0)}]|}. \end{aligned}$$

Finally, we compute the advection term as

$$\begin{aligned}
\langle \mathbf{d} \, i_v \omega_d^{(2)}, \star[\sigma_i^{(0)}] \rangle &= \langle i_v \omega_d^{(2)}, \partial \star[\sigma_i^{(0)}] \rangle = \langle \star(\star \omega_d^{(2)} \wedge v^{b_{dpp}}), \partial \star[\sigma_i^{(0)}] \rangle \\
&= \langle \star(\star \omega_d^{(2)} \wedge v^{b_{dpp}}), (-1) \star \star \partial \star[\sigma_i^{(0)}] \rangle \\
&= (-1) \frac{|\partial \star \sigma_i^{(0)}|}{|\star \partial \star[\sigma_i^{(0)}]|} \langle \star \omega_d^{(2)} \wedge v^{b_{dpp}}, \star \partial \star[\sigma_i^{(0)}] \rangle \\
&= (-1) \sum_{[\sigma_i^{(0)}] \prec [\sigma_k^{(0)}, \sigma_i^{(0)}]} \frac{|\star[\sigma_i^{(0)}] \cap \star[\sigma_k^{(0)}]|}{|[\sigma_k^{(0)}, \sigma_i^{(0)}]|} \langle \star \omega_d^{(2)} \wedge v^{b_{dpp}}, [\sigma_k^{(0)}, \sigma_i^{(0)}] \rangle.
\end{aligned}$$

Now, we can replace the usual wedge product \wedge by \wedge_{up} , use (11) and observe that, due to our geometric construction, we have

$$\frac{|[\sigma_i^{(0)}, \sigma_k^{(0)}] \cap \star[\sigma_k^{(0)}]|}{|[\sigma_i^{(0)}, \sigma_k^{(0)}]|} = \frac{1}{2}.$$

Thus, we derived

$$\begin{aligned}
&(-1) \langle \mathbf{d} \, i_v \omega_d^{(2)}, \star[\sigma_i^{(0)}] \rangle \\
&= \sum_{[\sigma_i^{(0)}] \prec [\sigma_k^{(0)}, \sigma_i^{(0)}]} \frac{|\star[\sigma_i^{(0)}] \cap \star[\sigma_k^{(0)}]|}{|[\sigma_k^{(0)}, \sigma_i^{(0)}]|} \langle \star \omega_d^{(2)} \wedge_{\text{up}} v^{b_{dpp}}, [\sigma_k^{(0)}, \sigma_i^{(0)}] \rangle \\
&= \sum_{[\sigma_i^{(0)}] \prec [\sigma_k^{(0)}, \sigma_i^{(0)}]} \frac{|\star[\sigma_i^{(0)}] \cap \star[\sigma_k^{(0)}]|}{|[\sigma_k^{(0)}, \sigma_i^{(0)}]|} \left([r_{k,i}^{(1)} \langle v^{b_{dpp}}, [\sigma_k^{(0)}, \sigma_i^{(0)}] \rangle \langle \star \omega_d^{(2)}, [\sigma_i^{(0)}] \rangle \right. \\
&\quad \left. - [(1 - r_{k,i}^{(1)}) \langle v^{b_{dpp}}, [\sigma_i^{(0)}, \sigma_k^{(0)}] \rangle \langle \star \omega_d^{(2)}, [\sigma_k^{(0)}] \rangle] \right).
\end{aligned}$$

For the evaluation of the dual-primal-primal flat operator, we use definition (12). We then have

$$\begin{aligned}
\langle v^{b_{dpp}}, [\sigma_i^{(0)}, \sigma_k^{(0)}] \rangle &= \sum_{\sigma^{(2)} \succ [\sigma_i^{(0)}, \sigma_k^{(0)}]} \frac{|\star[\sigma_i^{(0)}] \cap \star[\sigma_k^{(0)}] \cap \sigma^{(2)}|}{|\star[\sigma_i^{(0)}] \cap \star[\sigma_k^{(0)}]|} (\mathbf{v}(\sigma^{(2)}) \cdot (\sigma_k^{(0)} - \sigma_i^{(0)})) \\
\langle v^{b_{dpp}}, [\sigma_k^{(0)}, \sigma_i^{(0)}] \rangle &= \sum_{\sigma^{(2)} \succ [\sigma_k^{(0)}, \sigma_i^{(0)}]} \frac{|\star[\sigma_k^{(0)}] \cap \star[\sigma_i^{(0)}] \cap \sigma^{(2)}|}{|\star[\sigma_k^{(0)}] \cap \star[\sigma_i^{(0)}]|} (\mathbf{v}(\sigma^{(2)}) \cdot (\sigma_i^{(0)} - \sigma_k^{(0)})) \\
&= -\langle v^{b_{dpp}}, [\sigma_i^{(0)}, \sigma_k^{(0)}] \rangle,
\end{aligned}$$

where we understand \mathbf{v} to be piecewise constant on each primal 2-simplex. Furthermore, we stress the similarity to the finite volume scheme by abbreviating

$$\gamma_{k,i} := \sum_{\sigma^{(2)} \succ [\sigma_k^{(0)}, \sigma_i^{(0)}]} \frac{|\star[\sigma_i^{(0)}] \cap \star[\sigma_k^{(0)}] \cap \sigma^{(2)}|}{|\star[\sigma_i^{(0)}] \cap \star[\sigma_k^{(0)}]|} \frac{1}{|\sigma_k^{(0)} - \sigma_i^{(0)}|} \mathbf{v}(\sigma^{(2)}) \cdot (\sigma_k^{(0)} - \sigma_i^{(0)}).$$

Now, we can define the function $r^{(1)} : \mathbb{R} \rightarrow [0, 1]$ by setting

$$r^{(1)}(z) := \begin{cases} \frac{1}{2}, & \text{central differences} \\ \frac{1}{2}(\text{sgn}(z) + 1), & \text{full upwind.} \end{cases} \quad (23)$$

We set

$$r_{k,i}^{(1)} := r^{(1)} \left(\frac{\gamma_{k,i} |\sigma_i^{(0)}, \sigma_k^{(0)}|}{\alpha} \right). \quad (24)$$

The term $\frac{\gamma_{k,i} |\sigma_i^{(0)}, \sigma_k^{(0)}|}{\alpha}$ is called local Péclet number.

An other choice for the function $r^{(1)}(z)$ defined in [KA03, Section 8.2] is:

$$r^{(1)}(z) := 1 - \frac{1}{z} \left(1 - \frac{z}{e^z - 1} \right) \quad \text{exponential upwind} \quad (25)$$

We obtain for the case of central differences, i.e. $r^{(1)} := \frac{1}{2}$

$$\begin{aligned} & \langle \mathbf{d} \mathbf{i}_v \omega_d^{(2)}, \star[\sigma_i^{(0)}] \rangle \\ &= (-1) \sum_{[\sigma_i^{(0)}] \prec [\sigma_k^{(0)}, \sigma_i^{(0)}]} \frac{1}{2} \frac{|\star[\sigma_i^{(0)}] \cap \star[\sigma_k^{(0)}]|}{|[\sigma_k^{(0)}, \sigma_i^{(0)}]|} \left((-1) \langle v^{\flat dpp}, [\sigma_i^{(0)}, \sigma_k^{(0)}] \rangle \langle \star \omega_d^{(2)}, [\sigma_i^{(0)}] \rangle \right. \\ & \quad \left. - \langle v^{\flat dpp}, [\sigma_i^{(0)}, \sigma_k^{(0)}] \rangle \langle \star \omega_d^{(2)}, [\sigma_k^{(0)}] \rangle \right) \\ &= \sum_{[\sigma_i^{(0)}] \prec [\sigma_k^{(0)}, \sigma_i^{(0)}]} \frac{|\star[\sigma_i^{(0)}] \cap \star[\sigma_k^{(0)}]|}{2 |[\sigma_k^{(0)}, \sigma_i^{(0)}]|} \langle v^{\flat dpp}, [\sigma_i^{(0)}, \sigma_k^{(0)}] \rangle \left(\langle \star \omega_d^{(2)}, [\sigma_k^{(0)}] \rangle + \langle \star \omega_d^{(2)}, [\sigma_i^{(0)}] \rangle \right) \\ &= \sum_{[\sigma_i^{(0)}] \prec [\sigma_k^{(0)}, \sigma_i^{(0)}]} \gamma_{k,i} |\star[\sigma_i^{(0)}] \cap \star[\sigma_k^{(0)}]| \left(\frac{1}{2} \langle \star \omega_d^{(2)}, [\sigma_k^{(0)}] \rangle + \frac{1}{2} \langle \star \omega_d^{(2)}, [\sigma_i^{(0)}] \rangle \right). \end{aligned}$$

Finally, we obtain

$$\begin{aligned} & \langle \mathbf{d} \mathbf{i}_v \omega_d^{(2)}, \star \sigma_i^{(0)} \rangle = \\ &= \sum_{[\sigma_i^{(0)}] \prec [\sigma_k^{(0)}, \sigma_i^{(0)}]} \gamma_{k,i} |\star[\sigma_i^{(0)}] \cap \star[\sigma_k^{(0)}]| \left(\frac{1}{2} \langle \star \omega_d^{(2)}, [\sigma_k^{(0)}] \rangle + \frac{1}{2} \langle \star \omega_d^{(2)}, [\sigma_i^{(0)}] \rangle \right). \end{aligned}$$

Collecting the terms yields the claim. \square

4.2 Relation to Finite Differences

Next, we consider the setting of the discrete Lie advection for differential 0-forms in the two-dimensional case.

We use the finite differences approximation as defined in [GDN97, 3.2-3.5] to discretize (13). We employ a regular (square) grid for finite differences and get for a vertex $x_i \in \mathbb{R}^2$ on the grid with neighbors $x_i^N, x_i^S, x_i^W, x_i^E$ and edge length h

$$\begin{aligned} & -\alpha_i \frac{u(x_i^N) + u(x_i^S) + u(x_i^W) + u(x_i^E) - 4u(x_i)}{h^2} \\ & -v_x \frac{u(x_i^W) - u(x_i^E)}{2h} - v_y \frac{u(x_i^S) - u(x_i^N)}{2h} \\ & +cu(x_i) = f(x_i), \end{aligned} \quad (26)$$

where we refer for the notation to [GDN97, 3.2-3.5]. Here, we applied central differences for the discretizations of the first derivatives.

Equivalence to the DEC method

To compare this scheme with the DEC, we use a rectangular regular grid as primal grid, and calculate a well-centered dual rectangular regular grid which is again a regular grid shifted by $\frac{h}{2}$ in x and y direction. This is usually called staggered grid construction. The main geometric properties, e.g. that dual 1-simplices (edges) are perpendicular to the corresponding primal 1-simplices (edges) and that dual edges intersect themselves at the circumcenter of the primal 2-simplex, still hold on rectangular grids.

Theorem 2. *Let $\omega_p^{(0)}, \eta^{(0)} \in C^0(K)$ be primal 0-forms, $\alpha \geq 0$ and $c \in \mathbb{R}$ given constants and $\mathbf{v} : |\star K| \rightarrow \mathbb{R}^2$ a vector field. We consider*

$$\alpha \langle \star \mathbf{d} \star \mathbf{d} \omega_p^0, \sigma_i^{(0)} \rangle + \langle \mathbf{i}_v \mathbf{d} \omega_p^{(0)}, \sigma_i^{(0)} \rangle + c \langle \omega_p^{(0)}, \sigma_i^{(0)} \rangle = \langle \eta^0, \sigma_i^{(0)} \rangle. \quad (27)$$

By setting $u := \omega_p^0$, $f = \eta^0$ and $r_{i,j} = \frac{1}{2}$, we get that (27) is equivalent to (14).

Proof. We have by definition $\langle \omega^{(0)}, \sigma_i^{(0)} \rangle = \omega^{(0)}(\sigma_i^{(0)})$. Analogue calculations yield $c \langle \omega^0, \sigma_i^{(0)} \rangle = c \omega^{(0)}(\sigma_i^{(0)})$ and $\langle \eta^0, \sigma_i^{(0)} \rangle = c \eta^{(0)}(\sigma_i^{(0)})$. For the diffusion term, we get

$$\begin{aligned}
\langle \star \mathbf{d} \star \mathbf{d} \omega^0, [\sigma_i^{(0)}] \rangle &= \frac{1}{|\star \sigma_i^{(0)}|} \langle \mathbf{d} \star \mathbf{d} \omega^0, \star [\sigma_i^{(0)}] \rangle = \frac{1}{|\star \sigma_i^{(0)}|} \langle \star \mathbf{d} \omega^0, \partial \star [\sigma_i^{(0)}] \rangle \\
&= \frac{(-1)}{|\star \sigma_i^{(0)}|} \langle \star \mathbf{d} \omega^0, \star \star \partial \star [\sigma_i^{(0)}] \rangle \\
&= \frac{(-1)}{|\star \sigma_i^{(0)}|} \sum_{[\sigma_i^{(0)}] \prec [\sigma_k^{(0)}, \sigma_i^{(0)}]} \frac{|\star [\sigma_k^{(0)}] \cap \star [\sigma_i^{(0)}]|}{|[\sigma_k^{(0)}, \sigma_i^{(0)}]|} \langle \mathbf{d} \omega^0, [\sigma_k^{(0)}, \sigma_i^{(0)}] \rangle \\
&= \frac{(-1)}{|\star \sigma_i^{(0)}|} \sum_{[\sigma_i^{(0)}] \prec [\sigma_k^{(0)}, \sigma_i^{(0)}]} \frac{|\star [\sigma_k^{(0)}] \cap \star [\sigma_i^{(0)}]|}{|[\sigma_k^{(0)}, \sigma_i^{(0)}]|} \langle \omega^0, \partial [\sigma_k^{(0)}, \sigma_i^{(0)}] \rangle \\
&= \frac{(-1)}{|\star \sigma_i^{(0)}|} \sum_{[\sigma_i^{(0)}] \prec [\sigma_k^{(0)}, \sigma_i^{(0)}]} \frac{|\star [\sigma_k^{(0)}] \cap \star [\sigma_i^{(0)}]|}{|[\sigma_k^{(0)}, \sigma_i^{(0)}]|} \left(\langle \omega^0, [\sigma_k^{(0)}] \rangle - \langle \omega^0, [\sigma_i^{(0)}] \rangle \right).
\end{aligned}$$

With a regular square grid, we have

$$|\star \sigma_i^{(0)}| = h^2 \quad \text{and} \quad \frac{|\star [\sigma_k^{(0)}] \cap \star [\sigma_i^{(0)}]|}{|[\sigma_k^{(0)}, \sigma_i^{(0)}]|} = \frac{h}{h} = 1,$$

where $h > 0$ denotes the mesh-width of the grid. For the advection term, we have to consider $\langle \mathbf{i}_v \mathbf{d} \omega_p^{(0)}, [\sigma_i^{(0)}] \rangle$. Here, we employ the more geometrically motivated expression from [Hir03, p. 93] (see also Theorem 3) for the contraction using the notion of extrusions. We first observe that we have (subscripts denote horizontal and vertical components of a vector)

$$\begin{aligned}
\mathbf{v} &:= v_{\text{hor}} \mathbf{e}_1 + v_{\text{vert}} \mathbf{e}_2 \\
&= \frac{1}{2h} \left(v_{\text{hor}} (\sigma_{i,N}^{(0)} - \sigma_i^{(0)}) + v_{\text{hor}} (\sigma_i^{(0)} - \sigma_{i,S}^{(0)}) \right) \\
&\quad + \frac{1}{2h} \left(v_{\text{vert}} (\sigma_{i,E}^{(0)} - \sigma_i^{(0)}) + v_{\text{vert}} (\sigma_i^{(0)} - \sigma_{i,W}^{(0)}) \right).
\end{aligned}$$

Hence, we obtain with

$$\begin{aligned}
2h \langle \mathbf{i}_v \mathbf{d} \omega_p^{(0)}, [\sigma_i^{(0)}] \rangle &= \\
&= v_{\text{hor}} \left(\langle \mathbf{d} \omega_p^{(0)}, [\sigma_{i,N}^{(0)}, \sigma_i^{(0)}] \rangle + \langle \mathbf{d} \omega_p^{(0)}, [\sigma_i^{(0)}, \sigma_{i,S}^{(0)}] \rangle \right) \\
&\quad + v_{\text{vert}} \left(\langle \mathbf{d} \omega_p^{(0)}, [\sigma_{i,E}^{(0)}, \sigma_i^{(0)}] \rangle + \langle \mathbf{d} \omega_p^{(0)}, [\sigma_i^{(0)}, \sigma_{i,W}^{(0)}] \rangle \right).
\end{aligned}$$

Collecting the terms yields the final assertion. \square

5 Numerical Experiments

Since we work in the DEC-setting, the objects we study are not functions but discrete differential forms. This implies that we work with vectors as in (4) for primal 0-forms and dual 2-forms. We identify a 0-form with a function $\omega_p^0 \leftrightarrow w^0 : |K|_{\text{sp}} \rightarrow \mathbb{R}$ and a dual 2-form with $\omega_d^2 \leftrightarrow w^2 dx dy$. Moreover, each σ_j^0 with $1 \leq j \leq N_0$ and N_0 defined in (3) is just a primal vertex for which we use the same notation. This yields

$$\begin{aligned} \mathcal{C}^0(K) \ni \omega_p^0 &\leftrightarrow (\langle \omega_p^0, \sigma_1^0 \rangle, \dots, \langle \omega_p^0, \sigma_{N_0}^0 \rangle)^\top \in \mathbb{R}^{N_0} \\ &= \Omega_p^0 := (w^0(\sigma_1^0), \dots, w^0(\sigma_{N_0}^0))^\top \\ \mathcal{C}^2(\star K) \ni \omega_d^2 &\leftrightarrow (\langle \omega_d^2, \star \sigma_1^0 \rangle, \dots, \langle \omega_d^2, \star \sigma_{N_0}^0 \rangle)^\top \in \mathbb{R}^{N_0} \\ &\approx \Omega_d^2 := (|\star \sigma_1^0| w^2(\sigma_1^0), \dots, |\star \sigma_{N_0}^0| w^2(\sigma_{N_0}^0))^\top, \end{aligned}$$

where the last approximation corresponds to a mid-point quadrature rule. Note that on a square mesh with side-length h we have $|\star \sigma_j^0| = h^2$ for all $1 \leq j \leq N_0$. We measure the distances in a discrete L^2 -norm, that is

$$\begin{aligned} \|\omega_p^0 - \tilde{\omega}_p^0\|_{L^2_{\mathcal{C}^0(K)}}^2 &:= \frac{1}{N_0} \sum_{i=1}^{N_0} (w^0(\sigma_i^0) - \tilde{w}^0(\sigma_i^0))^2 \\ &= (\Omega_p^0 - \tilde{\Omega}_p^0)^\top \text{diag}(N_0^{-1}) (\Omega_p^0 - \tilde{\Omega}_p^0) \\ \|\omega_d^2 - \tilde{\omega}_d^2\|_{L^2_{\mathcal{C}^2(\star K)}}^2 &:= \frac{1}{N_0} \sum_{i=1}^{N_0} (w^2(\sigma_i^0) - \tilde{w}^2(\sigma_i^0))^2 \\ &= (\Omega_d^2 - \tilde{\Omega}_d^2)^\top \text{diag}(|\star \sigma_1^0|^{-1} N_0^{-1}) (\Omega_d^2 - \tilde{\Omega}_d^2) \end{aligned} \quad (28)$$

This norm is used to indicate the error in the numerical experiments.

5.1 Pure Advection on a flat regular mesh

We work in the setting of Theorem 1, i.e., we consider the advection for a dual 2-form and discretize the spatial operators as outlined there. We set $u(\cdot, t) := w^2(t)$ in the notation of (28). The discrete 1-form corresponding to a vector field \mathbf{v} reads $\langle \mathbf{v}^b, \mathbf{e} \rangle = \frac{1}{|\mathbf{e}|}$ for each edge \mathbf{e} , because all edges are axis-aligned either in positive x or y direction. As already mentioned, the rectangular grid has the same properties¹ as a well-centered triangulation and the dual grid is just a shifted rectangular grid. The flat operator mapping vectors to 1-forms can be implemented via splitting by dimension. This way, we can use rectangular grids for our experiments. We compare the standard DEC (central) scheme with our full upwind scheme, see (23). Hence,

¹ e.g. orthogonality of primal and dual edges

as a first example, we consider the PDE

$$\nabla \cdot (\mathbf{v}(x)u(\mathbf{x},t)) = \frac{\partial u}{\partial t}(\mathbf{x},t) \quad \text{for } \mathbf{x} = (x,y)^\top \in \Omega = [0,1]^2, \quad (29)$$

i.e., a pure advection of the concentration u with the vector field \mathbf{v} . For the time-integration, we use an (explicit) Euler scheme with $\delta t = 0.5h^2$ such that the CFL condition holds. While the CFL condition would only require a time-step $\delta t < h/|\mathbf{v}|$, we need to use here a time-step which is quadratic instead in h to show the second order rate of the central derivatives.

We consider as initial data a smooth Gaussian-like function (see Figure 4), as defined by

$$u_0(x,y) = u(x,y,0) = \exp(1) \exp\left(-\frac{1}{(1-\hat{x}^2)(1-\hat{y}^2)}\right), \quad (30)$$

where we set $\hat{x} = 2x - 1, \hat{y} = 2y - 1$ to center the function at $(0.5, 0.5)$. We set $\mathbf{v} = (1, 1)^\top$ and $T = 1.0$ on a square grid on $\Omega = [0, 1]^2$ with cells of size $h \times h$ with periodic boundary conditions. The choices imply that the initial condition u_0 will be recovered at time $T = 1$, i.e., $u(x,y,1) = u_0(x,y)$. As error measure we employ the difference between the analytic function and the result in the norm defined in (28). Precisely, we consider $u(\cdot, 0) = u_0 \leftrightarrow \omega_d^2$ and $u(\cdot, 1) \approx u(\cdot, 1) \leftrightarrow \tilde{\omega}_d^2$.

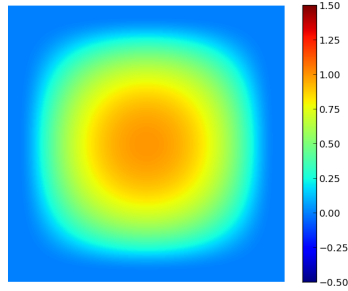


Fig. 4: Initial condition

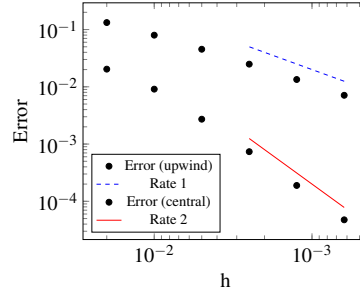


Fig. 5: Convergence rates of the advected concentration.

Figure 5 and Table 1 shows the error $\|\omega_d^2 - \tilde{\omega}_d^2\|_{L^2_{C^2(\star K)}}$. We observe an asymptotic rate of one for our upwind approach and a rate of two for the standard DEC approach, when the central scheme is in a stable regime.

5.2 Advection of Zalesak's Disc

Next, we consider an analogue problem to (29) but with non-smooth initial data u_0 . We use Zalesak's disc (see [LSM10, Section 5]) of radius 0.2 centered at $(0.5, 0.5)$

Table 1: Error versus mesh width h between the initial values and the advected function at time T . We achieve a rate of ≈ 0.915 for our upwind scheme and a rate of ≈ 1.993 with the central scheme.

h	Error (upwind)	h	Error (central)
$2.00 \cdot 10^{-2}$	$1.33 \cdot 10^{-1}$	$2.00 \cdot 10^{-2}$	$2.03 \cdot 10^{-2}$
$1.00 \cdot 10^{-2}$	$7.98 \cdot 10^{-2}$	$1.00 \cdot 10^{-2}$	$9.10 \cdot 10^{-3}$
$5.00 \cdot 10^{-3}$	$4.53 \cdot 10^{-2}$	$5.00 \cdot 10^{-3}$	$2.72 \cdot 10^{-3}$
$2.50 \cdot 10^{-3}$	$2.49 \cdot 10^{-2}$	$2.50 \cdot 10^{-3}$	$7.36 \cdot 10^{-4}$
$1.25 \cdot 10^{-3}$	$1.34 \cdot 10^{-2}$	$1.25 \cdot 10^{-3}$	$1.89 \cdot 10^{-4}$
$6.25 \cdot 10^{-4}$	$7.11 \cdot 10^{-3}$	$6.25 \cdot 10^{-4}$	$4.75 \cdot 10^{-5}$

on the unit square (see Figure 6) as initial data and employ a rotational vector field

$$\mathbf{v}(x,y) = \begin{pmatrix} (0.5-y) \\ (x-0.5) \end{pmatrix}.$$

The results are shown in Figure 6. We compare the solution after one full rota-

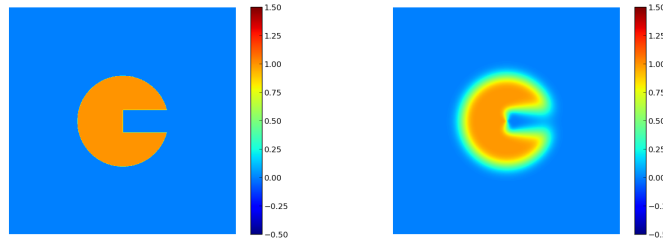


Fig. 6: left: Initial condition, i.e., Zalesak's disc of radius 0.2 centered at $(0.5, 0.5)$. right: after one full rotation on a mesh with 800×800 cells.

tion around the center of the square with the initial condition. We observe a slight smearing out of the boundary of the disc, which is due to the low order of polynomial exactness of (11). Moreover, we see in Figure 7 a convergence rate of ≈ 0.259 for our upwind scheme and a rate of ≈ 0.302 for the central scheme as the grid is refined. The rates are worse than in the smooth case in Section 5.1 due to the non-smooth initial condition, but the observed rates match the results from the literature for the rotation of Zalesak's disc nevertheless quite well, cf. [LSM10].

Table 2: Errors after a full rotation of Zalesak's disc.

h	Error (central)
$2.00 \cdot 10^{-2}$	$1.26 \cdot 10^{-1}$
$1.00 \cdot 10^{-2}$	$9.45 \cdot 10^{-2}$
$5.00 \cdot 10^{-3}$	$7.70 \cdot 10^{-2}$
$2.50 \cdot 10^{-3}$	$6.21 \cdot 10^{-2}$
$1.25 \cdot 10^{-3}$	$5.04 \cdot 10^{-2}$

h	Error (upwind)
$2.00 \cdot 10^{-2}$	$1.96 \cdot 10^{-1}$
$1.00 \cdot 10^{-2}$	$1.67 \cdot 10^{-1}$
$5.00 \cdot 10^{-3}$	$1.40 \cdot 10^{-1}$
$2.50 \cdot 10^{-3}$	$1.17 \cdot 10^{-1}$
$1.25 \cdot 10^{-3}$	$9.78 \cdot 10^{-2}$

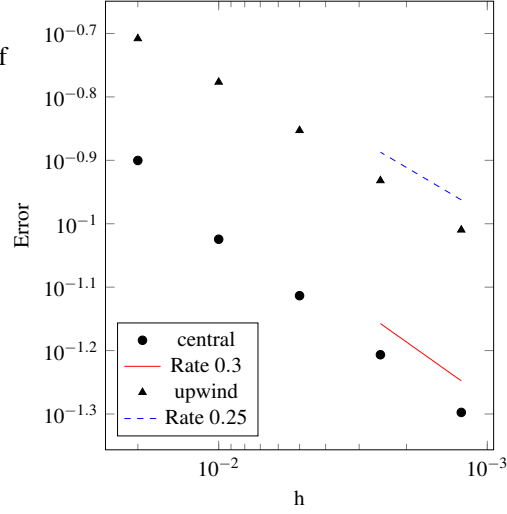


Fig. 7: The convergence rates after a full rotation of Zalesak's disc.

5.3 Advection-Diffusion convergence rates

Now, we deal with an advection-diffusion problem. As in Section 5.1, we work in the setting of Theorem 1, i.e., we consider the advection for a dual 2-form and discretize the spatial operators as outlined there. Again, we set $u(\cdot, t) := w^2(t)$ and the discrete 1-form corresponding to a vector field \mathbf{v} reads $\langle \mathbf{v}^b, \mathbf{e} \rangle = \frac{1}{|\mathbf{e}|}$ for each edge \mathbf{e} . We solve the equation

$$\frac{\partial u}{\partial t} - \alpha \Delta u + \nabla \cdot (\mathbf{v}u) = f$$

on $[0, 1]^2$ with periodic boundary conditions and $\mathbf{v} = (1, 1)^T$. As right hand side we choose

$$\begin{aligned} f(x, y, t) := & -v_x 2\pi \cos(2\pi(x - tv_x)) \sin(2\pi(y - tv_y)) \\ & -v_y 2\pi \sin(2\pi(x - tv_x)) \cos(2\pi(y - tv_y)) \\ & + 2\pi \cos(2\pi(x - tv_x)) \sin(2\pi(y - tv_y)) \\ & + 2\pi \sin(2\pi(x - tv_x)) \cos(2\pi(y - tv_y)) \\ & + \alpha 8\pi^2 \sin(2\pi(x - tv_x)) \sin(2\pi(y - tv_y)). \end{aligned} \quad (31)$$

This leads to an analytical solution in closed form

$$u(x, y, t) = \sin(2\pi(x - tv_x)) \sin(2\pi(y - tv_y)).$$

As time-integrator, we employ as in Section 5.1 the explicit Euler scheme with a time-step of $\delta t = \frac{h^2}{2}$. This allows for second order convergence although the time integrator is only of first order. Since we expect convergence rates ranging from first to second order, we use the exponential upwind coefficient depending on the local Péclet number as in (25). In the case of pure diffusion the coefficients simplify to the central differences scheme. Furthermore, one sided differences (full upwind) are recovered for $\alpha \rightarrow 0$.

For the convergence study, we make use of the fact that we have an analytical solution available. The error is measured after N time-steps, i.e, at time $T = N \cdot \delta t$ for different diffusion coefficients $\alpha \geq 0$. The results are shown in Figure 8 and Table 3. We clearly see the expected behavior, namely that we are able to smoothly vary the scheme (and the convergence rates) depending on the Péclet number.

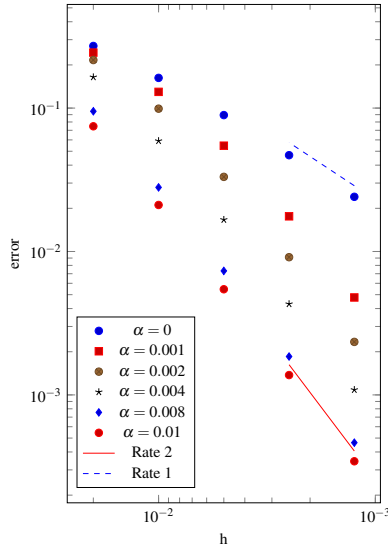


Fig. 8: Convergence rates for different diffusion coefficients α with the upwind scheme from (25) at time $t = 1.0$.

Table 3: The errors for different diffusion coefficients α with the Péclet number depending upwind scheme from (25) at time $t = 1.0$.

$\alpha = 0.0$		$\alpha = 0.001$	
h	Error	h	Error
$2.00 \cdot 10^{-2}$	$2.71 \cdot 10^{-1}$	$2.00 \cdot 10^{-2}$	$2.44 \cdot 10^{-1}$
$1.00 \cdot 10^{-2}$	$1.62 \cdot 10^{-1}$	$1.00 \cdot 10^{-2}$	$1.30 \cdot 10^{-1}$
$5.00 \cdot 10^{-3}$	$8.94 \cdot 10^{-2}$	$5.00 \cdot 10^{-3}$	$5.47 \cdot 10^{-2}$
$2.50 \cdot 10^{-3}$	$4.69 \cdot 10^{-2}$	$2.50 \cdot 10^{-3}$	$1.76 \cdot 10^{-2}$
$1.25 \cdot 10^{-3}$	$2.41 \cdot 10^{-2}$	$1.25 \cdot 10^{-3}$	$4.78 \cdot 10^{-3}$
$\alpha = 0.002$		$\alpha = 0.004$	
h	Error	h	Error
$2.00 \cdot 10^{-2}$	$2.16 \cdot 10^{-1}$	$2.00 \cdot 10^{-2}$	$1.64 \cdot 10^{-1}$
$1.00 \cdot 10^{-2}$	$9.91 \cdot 10^{-2}$	$1.00 \cdot 10^{-2}$	$5.90 \cdot 10^{-2}$
$5.00 \cdot 10^{-3}$	$3.31 \cdot 10^{-2}$	$5.00 \cdot 10^{-3}$	$1.67 \cdot 10^{-2}$
$2.50 \cdot 10^{-3}$	$9.13 \cdot 10^{-3}$	$2.50 \cdot 10^{-3}$	$4.31 \cdot 10^{-3}$
$1.25 \cdot 10^{-3}$	$2.34 \cdot 10^{-3}$	$1.25 \cdot 10^{-3}$	$1.09 \cdot 10^{-3}$
$\alpha = 0.008$		$\alpha = 0.01$	
h	Error	h	Error
$2.00 \cdot 10^{-2}$	$9.50 \cdot 10^{-2}$	$2.00 \cdot 10^{-2}$	$7.46 \cdot 10^{-2}$
$1.00 \cdot 10^{-2}$	$2.80 \cdot 10^{-2}$	$1.00 \cdot 10^{-2}$	$2.11 \cdot 10^{-2}$
$5.00 \cdot 10^{-3}$	$7.32 \cdot 10^{-3}$	$5.00 \cdot 10^{-3}$	$5.45 \cdot 10^{-3}$
$2.50 \cdot 10^{-3}$	$1.85 \cdot 10^{-3}$	$2.50 \cdot 10^{-3}$	$1.37 \cdot 10^{-3}$
$1.25 \cdot 10^{-3}$	$4.64 \cdot 10^{-4}$	$1.25 \cdot 10^{-3}$	$3.44 \cdot 10^{-4}$

5.4 Advection-Diffusion PDE on a curved mesh

As example of a smooth surface embedded into \mathbb{R}^3 , we consider the unit sphere. We triangulate a sphere with well-centered meshes using the program Comsol. It provided us with 9 different meshes with numbers of vertices ranging from 28, 64, 128, 234, 428, 656, 1408 to 3288. To have finer meshes, we refine thereafter the meshes by adding vertices at all edge midpoints and projecting the new points on the sphere. The meshes, we obtain that way, are well-centered in our cases.² Contrary to Section 5.1, we work here in the setting of Theorem 2, since we study $\mathbf{v} \cdot \nabla_S u$ instead of $\nabla_S \cdot (\mathbf{v}u)$. The differential equation we study is

$$\frac{\partial u}{\partial t} - \alpha \Delta_S u + \mathbf{v} \cdot \nabla_S u = 0, \quad \alpha \geq 0,$$

where the subscript S denotes the spherical differential operators. We use the discretization

$$\frac{\langle \omega_d^{(2)[n+1]}, \sigma_d^2 \rangle - \langle \omega_d^{(2)[n]}, \sigma_d^2 \rangle}{\delta t} + \left\langle \alpha \mathbf{d} \star \mathbf{d} \star \omega_d^{(2)[n]} + \star \mathbf{i}_v \mathbf{d} \star \omega_d^{(2)[n]}, \sigma_d^2 \right\rangle = 0. \quad (32)$$

With the choice $\sigma_d^2 = \star \sigma_i^{(0)}$ and $\omega_d^{(2)} = \star \omega_p^{(0)}$ this corresponds to Theorem 2. Here, we set $u(\cdot, t) := w^0(t)$ and the discrete 1-form corresponding to a vector field \mathbf{v} reads $\langle \mathbf{v}^b, \mathbf{e} \rangle = \frac{1}{|\mathbf{e}|}$ for each edge \mathbf{e} . We first employed a tangential vector field

$$\mathbf{v}(x, y, t) := \begin{pmatrix} -r \sin(\varphi) \cos(\theta) \\ r \cos(\varphi) \cos(\theta) \\ 0 \end{pmatrix}$$

where (r, φ, θ) are the spherical coordinates. Recall that we work on the unit sphere, i.e., $r = 1$.

In this experiment, we use the central scheme and the full upwind scheme, see (23). As time-integrator we again use the explicit Euler scheme with a time step of $\delta t = \min(h)^2/2$, where $h = \min(\sigma_d^1) \propto \text{diam}(T)$ for primal triangles T , such that the CFL condition holds. As initial condition, we use an exponential function

$$u_0(c(\sigma_d^2)) = \begin{cases} c_\phi & \text{for } d > r_a \\ c_\phi + e \cdot \exp\left(-\frac{1}{1-d^2}\right) & \text{else} \end{cases} \quad (33)$$

with $c(\sigma_d^2)$ as the center of the cell σ_d^2 , $d = \arccos(c(\sigma_d^2) \cdot (0, 1, 0)^T)$ as the spherical distance of the cell center to the center of mass and with parameters c_ϕ, r_a .

We choose $c_\phi = 2.0$, $r_a = 1.2$ and $\alpha = 0$ for the advection experiment, using the standard scheme³ and our upwind scheme.

² In general this algorithm does not guarantee well-centered meshes.

³ which is a weighted average of the finite differences scheme using adjacent vertices. This results on rectangular meshes indeed in the central difference scheme.

The result for the standard scheme is depicted in Figure 9. Note that we observe small oscillations due to the central difference scheme.

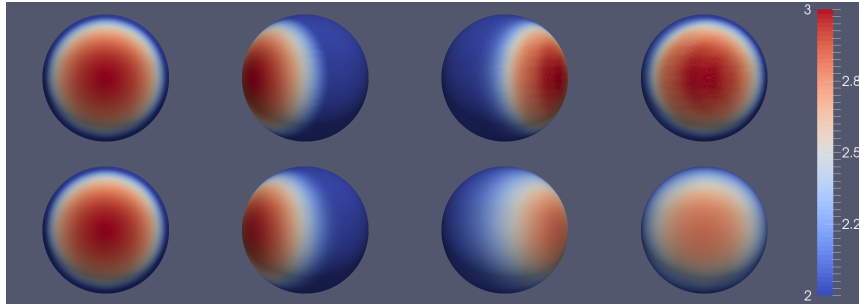


Fig. 9: Advection using the central scheme (top) and the novel upwind scheme (bottom) with a rotational vector field on the surface of a sphere with 13146 points: Concentration at the initial condition, after $\frac{1}{8}$ rotation, after $\frac{7}{8}$ rotation and for the final state

The convergence rate of the standard scheme and the upwind scheme for pure advection ($\alpha = 0$) is depicted in Figure 10 for the central difference scheme and in Figure 11 for the upwind scheme. From Table 4, we observe a rate of ≈ 2.015 with the standard scheme and from Table 5 a rate of ≈ 0.786 with our upwind scheme. The slightly reduced convergence rate might be due to the curved geometry.

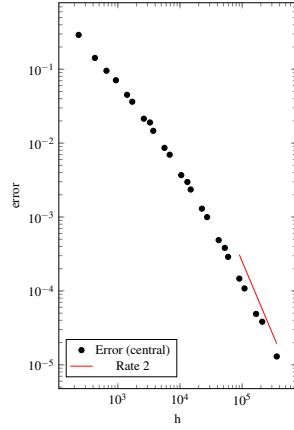


Fig. 10: Convergence rates after one rotation around the sphere.

Table 4: Error of the concentration in the dual cells after one rotation around the sphere.

Number of Points	Error (central)
$2.34 \cdot 10^2$	$2.92 \cdot 10^{-1}$
$4.28 \cdot 10^2$	$1.42 \cdot 10^{-1}$
$6.56 \cdot 10^2$	$9.55 \cdot 10^{-2}$
$9.30 \cdot 10^2$	$7.10 \cdot 10^{-2}$
$1.41 \cdot 10^3$	$4.51 \cdot 10^{-2}$
$1.71 \cdot 10^3$	$3.64 \cdot 10^{-2}$
$2.62 \cdot 10^3$	$2.14 \cdot 10^{-2}$
$3.29 \cdot 10^3$	$1.90 \cdot 10^{-2}$
$3.71 \cdot 10^3$	$1.47 \cdot 10^{-2}$
$5.63 \cdot 10^3$	$8.63 \cdot 10^{-3}$
$6.82 \cdot 10^3$	$6.97 \cdot 10^{-3}$
$1.05 \cdot 10^4$	$3.69 \cdot 10^{-3}$
$1.31 \cdot 10^4$	$2.98 \cdot 10^{-3}$
$1.49 \cdot 10^4$	$2.36 \cdot 10^{-3}$
$2.25 \cdot 10^4$	$1.30 \cdot 10^{-3}$
$2.73 \cdot 10^4$	$9.98 \cdot 10^{-4}$
$4.19 \cdot 10^4$	$4.87 \cdot 10^{-4}$
$5.26 \cdot 10^4$	$3.82 \cdot 10^{-4}$
$5.94 \cdot 10^4$	$2.89 \cdot 10^{-4}$
$9.00 \cdot 10^4$	$1.47 \cdot 10^{-4}$
$1.09 \cdot 10^5$	$1.08 \cdot 10^{-4}$
$1.67 \cdot 10^5$	$4.88 \cdot 10^{-5}$
$2.10 \cdot 10^5$	$3.83 \cdot 10^{-5}$
$3.60 \cdot 10^5$	$1.30 \cdot 10^{-5}$

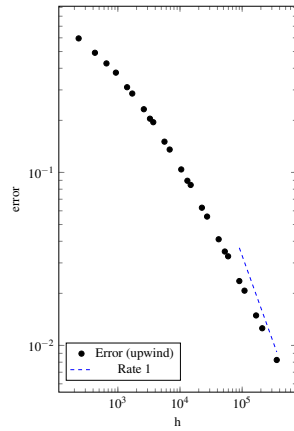


Fig. 11: Convergence rates after one rotation around the sphere.

Table 5: Error of the concentration in the dual cells after one rotation around the sphere.

Number of Points	Error (upwind)
$2.34 \cdot 10^2$	$5.95 \cdot 10^{-1}$
$4.28 \cdot 10^2$	$4.92 \cdot 10^{-1}$
$6.56 \cdot 10^2$	$4.27 \cdot 10^{-1}$
$9.30 \cdot 10^2$	$3.78 \cdot 10^{-1}$
$1.41 \cdot 10^3$	$3.11 \cdot 10^{-1}$
$1.71 \cdot 10^3$	$2.86 \cdot 10^{-1}$
$2.62 \cdot 10^3$	$2.32 \cdot 10^{-1}$
$3.29 \cdot 10^3$	$2.05 \cdot 10^{-1}$
$3.71 \cdot 10^3$	$1.95 \cdot 10^{-1}$
$5.63 \cdot 10^3$	$1.51 \cdot 10^{-1}$
$6.82 \cdot 10^3$	$1.36 \cdot 10^{-1}$
$1.05 \cdot 10^4$	$1.04 \cdot 10^{-1}$
$1.31 \cdot 10^4$	$8.95 \cdot 10^{-2}$
$1.49 \cdot 10^4$	$8.47 \cdot 10^{-2}$
$2.25 \cdot 10^4$	$6.25 \cdot 10^{-2}$
$2.73 \cdot 10^4$	$5.56 \cdot 10^{-2}$
$4.19 \cdot 10^4$	$4.11 \cdot 10^{-2}$
$5.26 \cdot 10^4$	$3.49 \cdot 10^{-2}$
$5.94 \cdot 10^4$	$3.28 \cdot 10^{-2}$
$9.00 \cdot 10^4$	$2.36 \cdot 10^{-2}$
$1.09 \cdot 10^5$	$2.07 \cdot 10^{-2}$
$1.67 \cdot 10^5$	$1.49 \cdot 10^{-2}$
$2.10 \cdot 10^5$	$1.26 \cdot 10^{-2}$
$3.60 \cdot 10^5$	$8.24 \cdot 10^{-3}$

6 Concluding Remarks and Outlook

We have introduced a upwind scheme based on the observation that the discrete exterior calculus coincides with classical numerical techniques in certain special cases. We have shown the stabilization effect and the numerical convergence properties of the resulting modified DEC method in Section 5.

Altogether, this is a first important step towards treating two-phase flow problems with a free surface on which a time-dependent advection-diffusion equation for the surfactant concentration is taken into account. But this application is still current work. Due to our new stabilized DEC approach, we are now able to cope with the stability issues of the advection equation on the free surface for general velocities of the fluid. Without a stabilization method, the DEC is surely doomed to fail in such applications as soon as there are larger flow velocities involved.

Finally, we shall give a few comments on further possible modifications of our numerical scheme. A major prerequisite for our new stabilized DEC scheme is the need of a well-centered mesh in the first place. Its construction in the general setting of curved surfaces is an issue and a challenging task for complex geometries. It is known since 1988 that there is a well-centered triangulation for every *planar* polygonal area [BGR88]. But the existence of well-centered triangulations for the curved case is much less clear. The same holds for its efficient algorithmic construction. Thus one may assume the weaker Delaunay property for which mesh generation is well-known. We expect that for the geometries which arise for e.g. bubbles in two phase flows, Delaunay triangulations are feasible and can be constructed without much problems. Our DEC scheme then needs to be slightly modified to account for negative volume of parts of the dual cell, when a dual vertex is the circumcenter of a non-well-centered triangle. Furthermore, a special boundary treatment for non-closed meshes [HKV13] needs to be added. Another possibility is the use of barycentric dual cells [AK06], though it is unclear if this is viable for the DEC since crucial features like the orthogonality of primal and dual edges are lost.

Appendix

Appendix A Derivation of the discrete contraction formula

In this section, we give a formal derivation of the formula for the discrete contraction. In contrast to [Hir03, p. 93] we obtain slightly different normalization factors. For the definitions see [Hir03].

Theorem 3. *For piecewise constant differential forms, ω^{k+1} is the evaluation of i_{σ^1} on a simplex σ^k with the algebraic definition from the geometric definition using the extrusion of σ^k equivalent to the evaluation of the discrete differential form on σ^{k+1} .*

Proof. We assume the differential form ω^{k+1} as piecewise constant on the $k+1$ -simplices which yields

$$\langle \omega^{k+1}, \text{extr}_{\sigma^1}(\sigma^k, t) \rangle = \frac{|\text{extr}_{\sigma^1}(\sigma^k, t)|}{|\sigma^{k+1}|} \langle \omega^{k+1}, \sigma^{k+1} \rangle.$$

Hence, we obtain

$$\begin{aligned} \langle i_v \omega^{k+1}, \sigma^k \rangle &:= \frac{d}{dt} \Big|_{t=0} \langle \omega^{k+1}, \text{extr}(\sigma^k, v_t) \rangle \\ &= \frac{d}{dt} \Big|_{t=0} \left(|\text{extr}_{\sigma^1}(\sigma^k, t)| \right) \frac{1}{|\sigma^{k+1}|} \langle \omega^{k+1}, \sigma^{k+1} \rangle. \end{aligned}$$

This shows that we have to consider the map $t \mapsto |\text{extr}_{\sigma^1}(\sigma^k, t)|$.

Following [Hir03, Chapter 8.3], we get

$$|\text{extr}_{\sigma^1}(\sigma^k, t)| = |\sigma^{k+1}| \frac{|h(t)|}{|h(1)|},$$

where σ^k is the base side of a $(k+1)$ -simplex and h its height. Here, we use the geometric definition and define the extrusion $\text{extr}_{\omega^1}(\sigma^k, t)$ of a face ω^k as the $(k+1)$ -simplex spanned by the face and a vector $\dot{\mathbf{x}}(t) = \sigma^1(1-t)$, $0 \leq t \leq 1$. We assume without loss of generality that the common vertex σ^0 of the face and the edge lies at the origin. Because we have $\dot{\mathbf{x}}(0) = 0$, we get $\mathbf{x}(t) = t - \frac{t^2}{2}$. The height is proportional to the edge $\sigma^1 = \mathbf{x}(1)$, spanning the $(k+1)$ -simplex together with the k -simplex σ^k . Thus, we have for $0 < t < 1$

$$\frac{h(t)}{h(1)} = \frac{|\mathbf{x}(t)|}{|\mathbf{x}(1)|} = \frac{|\sigma^1(t - \frac{t^2}{2})|}{|\sigma^1|} = t - \frac{t^2}{2}. \quad (34)$$

Hence, we obtain

$$\frac{d}{dt} \Big|_{t=0} \left(|\text{extr}_{\sigma^1}(\sigma^k, t)| \right) = 1 |\sigma^{k+1}|.$$

This yields the claim. \square

Acknowledgement

M. Griebel and A. Schier thank the *DFG* for the financial support through the *Priority Programme 1506: Transport Processes at Fluidic Interfaces* (SPP 1506). The authors would also like to thank B. Zwicknagl for reading parts of the manuscript and for inspiring discussions.

References

- AFW10. D. Arnold, R. Falk, and R. Winther, *Finite element exterior calculus: From Hodge theory to numerical stability*, Bulletin of the American Mathematical Society **47** (2010), no. 2, 281–354.
- AK06. B. Auchmann and S. Kurz, *A geometrically defined discrete Hodge operator on simplicial cells*, IEEE Transactions on Magnetics **42** (2006), no. 4, 643.
- Aur91. F. Aurenhammer, *Voronoi diagrams – a survey of a fundamental geometric data structure*, ACM Computing Surveys **23** (1991), no. 3, 345–405.
- Bey98. J. Bey, *Finite-Volumen- und Mehrgitterverfahren für elliptische Randwertprobleme*, Springer, 1998.
- BGR88. B. S. Baker, E. Grosse, and C. S. Rafferty, *Nonobtuse triangulation of polygons*, Discrete & Computational Geometry **3** (1988), no. 2, 147–168.
- BH. Nathan Bell and Anil N. Hirani, *PyDEC: Algorithms and software for Discretization of Exterior Calculus*.
- CGS09. R. Croce, M. Griebel, and M. A. Schweitzer, *Numerical simulation of bubble and droplet-deformation by a level set approach with surface tension in three dimensions*, International Journal for Numerical Methods in Fluids **62** (2009), no. 9, 963–993.
- DHLM05. M. Desbrun, A. N. Hirani, M. Leok, and J. E. Marsden, *Discrete exterior calculus*, arXiv preprint math/0508341, 2005.
- Ede98. H. Edelsbrunner, *Shape reconstruction with Delaunay complex*, LATIN’98: Theoretical Informatics: Third Latin American Symposium Campinas, Brazil, April 20–24, 1998 Proceedings (C. L. Lucchesi and A. V. Moura, eds.), Springer, Berlin Heidelberg, 1998, pp. 119–132.
- Ede01. ———, *Geometry and Topology for Mesh Generation*, Cambridge Univ. Press, Cambridge, England, 2001.
- Ede14. ———, *Roots of Geometry and Topology*, Springer International Publishing, 2014.
- EH10. H. Edelsbrunner and J. Harer, *Computational Topology. An Introduction*, Amer. Math. Soc., Providence, Rhode Island, 2010.
- GDN97. M. Griebel, T. Dornseifer, and T. Neunhoffer, *Numerical Simulation in Fluid Dynamics: A Practical Introduction*, Mathematical Modeling and Simulation, vol. 3, Siam, 1997.
- Heu11. H. Heumann, *Eulerian and semi-Lagrangian methods for advection-diffusion of differential forms*, Ph.D. thesis, Diss., Eidgenössische Technische Hochschule ETH Zürich, Nr. 19608, 2011.
- Hir03. A. N. Hirani, *Discrete exterior calculus*, Ph.D. thesis, California Institute of Technology, 2003.
- HKV13. A. N. Hirani, K. Kalyanaraman, and E. B. VanderZee, *Delaunay Hodge star*, Computer-Aided Design **45** (2013), no. 2, 540 – 544, Solid and Physical Modeling 2012.
- HNC15. Anil N. Hirani, Kalyana B. Nakshatrala, and Jehanzeb H. Chaudhry, *Numerical method for Darcy flow derived using Discrete Exterior Calculus*, International Journal for Computational Methods in Engineering Science & Mechanics **16** (2015), no. 3, 151–169.
- KA03. P. Knabner and L. Angermann, *Numerical Methods for Elliptic and Parabolic Partial Differential Equations*, Texts in Applied Mathematics, vol. 44, Springer, 2003.
- LSM10. Aymen Laadhari, Pierre Saramito, and Chaouqi Misbah, *Improving the mass conservation of the level set method in a finite element context*, Comptes Rendus Mathématique **348** (2010), no. 9, 535–540.
- MHR16. M. S. Mohamed, A. N. Hirani, and S. Ravi, *Discrete exterior calculus discretization of incompressible Navier–Stokes equations over surface simplicial meshes*, Journal of Computational Physics **312** (2016), 175 – 191.
- MMP⁺11. P. Mullen, A. McKenzie, D. Pavlov, L. Durant, Y. Tong, E. Kanso, J. E. Marsden, and M. Desbrun, *Discrete Lie advection of differential forms*, Foundations of Computational Mathematics **11** (2011), no. 2, 131–149.

- NNPV16. M. Nestler, I. Nitschke, S. Praetorius, and A. Voigt, *Orientalional order on surfaces - the coupling of topology, geometry and dynamics*, ArXiv e-prints (2016).
- NRV16. I. Nitschke, S. Reuther, and A. Voigt, *Discrete exterior calculus (DEC) for the surface Navier-Stokes equation*, ArXiv e-prints (2016).
- VHG⁺13. Evan VanderZee, Anil N. Hirani, Damrong Guoy, Vadim Zharnitsky, and Edgar Ramos, *Geometric and combinatorial properties of well-centered triangulations in three and higher dimensions*, *Computational Geometry: Theory and Applications* **46** (2013), no. 6, 700–724.